

Partial μ - τ Reflection Symmetry and Its Verification at DUNE and Hyper-Kamiokande

Kaustav Chakraborty^{1,2,*}, K. N. Deepthi^{1,†}, Srubabati Goswami^{1,‡}, Anjan S. Joshipura^{1,§} and Newton Nath^{3,4,¶}

¹Theoretical Physics Division, Physical Research Laboratory, Ahmedabad - 380009, India

²Discipline of Physics, Indian Institute of Technology, Gandhinagar - 382355, India

³Institute of High Energy Physics, Chinese Academy of Sciences, Beijing 100049, China

⁴School of Physical Sciences, University of Chinese Academy of Sciences, Beijing 100049, China

We study origin, consequences and testability of a hypothesis of ‘partial μ - τ ’ reflection symmetry. This symmetry predicts $|U_{\mu i}| = |U_{\tau i}|$ ($i = 1, 2, 3$) for a single column of the leptonic mixing matrix U . Depending on whether this symmetry holds for the first or second column of U different correlations between θ_{23} and δ_{CP} can be obtained. This symmetry can be obtained using discrete flavour symmetries. In particular, all the subgroups of $SU(3)$ with 3-dimensional irreducible representation which are classified as class C or D can lead to partial μ - τ reflection symmetry. We show how the predictions of this symmetry compare with the allowed area in the $\sin^2 \theta_{23} - \delta_{CP}$ plane as obtained from the global analysis of neutrino oscillation data. Furthermore, we study the possibility of testing these symmetries at the proposed DUNE and Hyper-Kamiokande (HK) experiments (T2HK, T2HKK), by incorporating the correlations between θ_{23} and δ_{CP} predicted by the symmetries. We find that when simulated data of DUNE and HK is fitted with the symmetry predictions, the $\theta_{23} - \delta_{CP}$ parameter space gets largely restricted near the CP conserving values of δ_{CP} . Finally, we illustrate the capability of these experiments to distinguish between the two cases leading to partial $\mu - \tau$ symmetry namely $|U_{\mu 1}| = |U_{\tau 1}|$ and $|U_{\mu 2}| = |U_{\tau 2}|$.

PACS numbers:

I. INTRODUCTION

Considerable theoretical and experimental efforts are being devoted towards predicting and determining the unknowns of the leptonic sectors namely CP violating phases, octant of the atmospheric mixing angle θ_{23} (i.e. $\theta_{23} < 45^\circ$, named as lower octant (LO) or $\theta_{23} > 45^\circ$ named as upper octant (HO)) and neutrino mass hierarchy (i.e. the sign of Δm_{31}^2 , $\Delta m_{31}^2 > 0$ known as normal hierarchy (NH) and $\Delta m_{31}^2 < 0$ known as inverted hierarchy (IH)). Symmetry based approaches have been quite successful in predicting the interrelations among these quantities and the structure of the leptonic mixing matrix as discussed in Refs. [1–5] and the references therein. General approaches along this line assume some individual residual symmetries of the leptonic mass matrices which could arise from the breaking of some bigger symmetry of the leptonic interactions. One such symmetry, called μ - τ reflection symmetry, originally discussed by Harrison and Scott in Ref. [6] leads to very successful predictions of mixing angles which are close to the present experimental knowledge and . This symmetry may be stated as equality of moduli of the leptonic mixing matrix U :

$$|U_{\mu i}| = |U_{\tau i}| , \quad (1)$$

for all the columns $i = 1, 2, 3$. Both the origin and consequences of this relation have been discussed in [7–22].

Using the standard PDG [23] parameterization of the matrix U

$$U = U(\theta_{23})U(\theta_{13}, \delta_{CP})U(\theta_{12})$$

$$= \begin{bmatrix} c_{12}c_{13} & s_{12}c_{13} & s_{13}e^{-i\delta_{CP}} \\ -s_{12}c_{23} - c_{12}s_{23}s_{13}e^{i\delta_{CP}} & c_{12}c_{23} - s_{12}s_{23}s_{13}e^{i\delta_{CP}} & s_{23}c_{13} \\ s_{12}s_{23} - c_{12}c_{23}s_{13}e^{i\delta_{CP}} & -c_{12}s_{23} - s_{12}c_{23}s_{13}e^{i\delta_{CP}} & c_{23}c_{13} \end{bmatrix} \quad (2)$$

*Email Address: kaustav@prl.res.in

†Email Address: deepthi@prl.res.in

‡Email Address: sruba@prl.res.in

§Email Address: anjan@prl.res.in

¶Email Address: newton@ihep.ac.cn

one finds two well-known predictions

$$\theta_{23} = \frac{\pi}{4}, \quad s_{13} \cos \delta_{CP} = 0. \quad (3)$$

This relation thus allows for a nonzero θ_{13} unlike the simple μ - τ symmetry which predicts vanishing θ_{13} [24–29], see recent review [30] and references therein. For $\theta_{13} \neq 0$, one gets $\delta_{CP} = \pm \frac{\pi}{2}$. Both these predictions are in accord with observations. The maximal θ_{23} is allowed within 1σ by the global fits to neutrino observables and $\delta_{CP} = -\frac{\pi}{2}$ is preferred by the T2K experiment [31] and global fit of all neutrino data [32–34]. However a sizable range is still allowed. Whereas, the best fit value of θ_{23} in the global fit deviates from the maximal value for either mass hierarchy. Such deviations can be regarded as a signal for the departure from the μ - τ reflection symmetry. A theoretically well-motivated possibility is to assume a ‘partial μ - τ ’ reflection symmetry [35] and assume that eq.(1) holds only for a single column¹ of U . Assuming that it holds for the third column, one gets maximal θ_{23} and δ_{CP} remains unrestricted. Eq.(1) on the other hand predicts correlations among δ_{CP} and mixing angles if it is true for any of the first two columns. These correlations are found from eq.(2) in respective cases $i = 1$ and $i = 2$ to be

$$\cos \delta_{CP} = \frac{(c_{23}^2 - s_{23}^2)(c_{12}^2 s_{13}^2 - s_{12}^2)}{4c_{12}s_{12}c_{23}s_{23}s_{13}}, \quad (|U_{\mu 1}| = |U_{\tau 1}|), \quad C_1, \quad (4)$$

$$\cos \delta_{CP} = \frac{(c_{23}^2 - s_{23}^2)(c_{12}^2 - s_{12}^2 s_{13}^2)}{4c_{12}s_{12}c_{23}s_{23}s_{13}}, \quad (|U_{\mu 2}| = |U_{\tau 2}|), \quad C_2. \quad (5)$$

These equations correlate the sign of $\cos \delta_{CP}$ to the octant of θ_{23} . θ_{23} in the first (second) octant leads to a negative (positive) value of $\cos \delta_{CP}$ in case of eq. (4). It predicts exactly opposite behavior for eq. (5). The exact quadrant of δ is still not fixed by these equations but it can also be determined from symmetry considerations [20]. These correlations were also obtained in [36, 37] in the context of Z_2 and $\overline{Z_2}$ symmetries². Henceforth we refer to these correlations as C_1 and C_2 respectively. The above equations also indirectly lead to information on the neutrino mass hierarchy since the best fit values of θ_{23} lie in the first (second) octant in case of the normal (inverted) hierarchy according to the latest global fits reported in [32–34]. Thus precise verification of the above equations is of considerable importance and the long baseline experiments can provide a way for such study. Similar study has been performed in the context of the NO ν A and T2K experiments in [39–41].

In this paper, we consider the testability of these relations at the forthcoming long baseline experiments Deep Under-ground Neutrino Experiment (DUNE) and Hyper-Kamiokande (HK). These potential high-statistics experiments will overcome the parameter degeneracies faced by the current experiments and lead us in to an era of precision measurements of the oscillation parameters [42–51]. Because of this, these experiments are ideal to test the parameter correlations like the ones given in eqs.(4, 5). In the following, we obtain the allowed parameter range in the $\delta_{CP} - \sin^2 \theta_{23}$ plane by fitting the above symmetry relations to the simulated DUNE and HK data. This in turn implies using the correlations embodied in the eqs. (4, 5) in the fit. We also discuss whether the correlations C_1 (eq. (4)) and C_2 (eq. (5)) can be distinguished at DUNE and HK. Recent studies on testing various models from future experiments can be found for instance in [52–60].

We begin by first discussing the origin of partial μ - τ reflection symmetry and discuss the robustness of the resulting predictions in a large class of models based on flavour symmetry in Section II. We give a brief overview of the experiments and simulation details in Section III. In Section IV, we perform a phenomenological analysis of the testability of the above symmetries in DUNE and HK. We use the extra correlations predicted by the symmetry in fitting the simulated data of these experiments and obtain the allowed areas in the $\delta_{CP} - \sin^2 \theta_{23}$ plane. In subsection IV B, we discuss the possibility of differentiating between the two correlations – C_1 and C_2 . We draw our conclusions in Section V.

II. PARTIAL μ - τ REFLECTION SYMMETRY AND DISCRETE FLAVOUR SYMMETRIES

We briefly review here the general approach based on flavour symmetry to emphasize that partial μ - τ reflection symmetry is a generic prediction of almost all such schemes barring few exceptions. Basic approaches assume groups G_ν and G_l as the residual symmetries of the neutrino mass matrix M_ν and the charged lepton mass matrix $M_l M_l^\dagger$ respectively. Both these groups are assumed to arise from the breaking of some unitary discrete group G_f . The U_{PMNS} matrix U gets fixed upto the neutrino Majorana phases if it is further assumed that $G_\nu = Z_2 \times Z_2$ and $G_l = Z_n, n \geq 3$. In addition, if we demand that all the predicted

¹ If it holds for any two columns then by unitarity, it holds for the third as well.

² See, the review article [38] for references on other similar sum rules and their testability.

mixing angles are non-zero, then the following unique form is predicted for almost all the discrete groups G_f [61, 62]

$$U \equiv U_{\text{gen}}(\theta_n) = \frac{1}{\sqrt{3}} \begin{pmatrix} \sqrt{2} \cos \theta_n & 1 & \sqrt{2} \sin \theta_n \\ \sqrt{2} \cos(\theta_n - \frac{2\pi}{3}) & 1 & \sqrt{2} \sin(\theta_n - \frac{2\pi}{3}) \\ \cos(\theta_n - \frac{4\pi}{3}) & 1 & \sqrt{2} \sin(\theta_n - \frac{4\pi}{3}) \end{pmatrix}, \quad (6)$$

where $\theta_n \equiv \frac{\pi a}{n}$ is a discrete angle with $a = 0, 1, 2, \dots, \frac{n}{2}$. We have not shown here the unphysical phases which can be absorbed in defining charged lepton fields and unpredicted Majorana phases. All the discrete subgroups of $SU(3)$ with three dimensional irreducible representation are classified as class C or D and five exceptional groups [63]. Eq.(6) follows in all the type D groups taken as G_f . Type C groups lead instead to democratic mixing which shows full μ - τ reflection symmetry but predict large reactor angle. Eq.(6) arises even if G_f is chosen as a discrete subgroup of $U(3)$ having the same textures as class D groups [62].

Eq.(6) displays partial μ - τ reflection symmetry for the second column for all the values of $\theta_n \neq 0, \frac{\pi}{2}$. In the latter case, one gets total μ - τ reflection symmetry but at the same time one of the mixing angles is predicted to be zero and one would need to break the assumed residual symmetries to get the correct mixing angles. More importantly, eq.(6) being essentially a real matrix also predicts trivial Dirac CP phase $\delta_{CP} = 0$ or π . Eq.(5) in this case implies a correlation among angles. Non-zero CP phase and partial μ - τ symmetry in other columns can arise in an alternative but less predictive approach in which the residual symmetry of the neutrino mass matrix is taken as Z_2 instead of $Z_2 \times Z_2$. In this case, one can obtain the following mixing matrix U with a proper choice of residual symmetries.

$$U = U_{\text{gen}}(0)U_{ij}, \quad (7)$$

where U_{ij} denotes a unitary rotation either in the ij^{th} plane corresponding to partial symmetry in the k^{th} $i \neq j \neq k$ column. Examples of the required residual symmetries are discussed in [1–5] and minimal example of this occurs with $G_f = S_4$.

The partial μ - τ symmetries obtained this way also lead to additional restrictions

$$c_{12}^2 c_{13}^2 = \frac{2}{3} \quad \text{or} \quad s_{12}^2 c_{13}^2 = \frac{1}{3}, \quad (8)$$

where the first (second) relation follows from the partial symmetries of the first(second) column. These predictions arise here from the requirement that G_ν and G_l are embedded in DSG of $SU(3)$ and need not arise in a more general approach. It is then possible to obtain specific symmetries [36, 37] in which solar angle is a function of a continuous parameter.

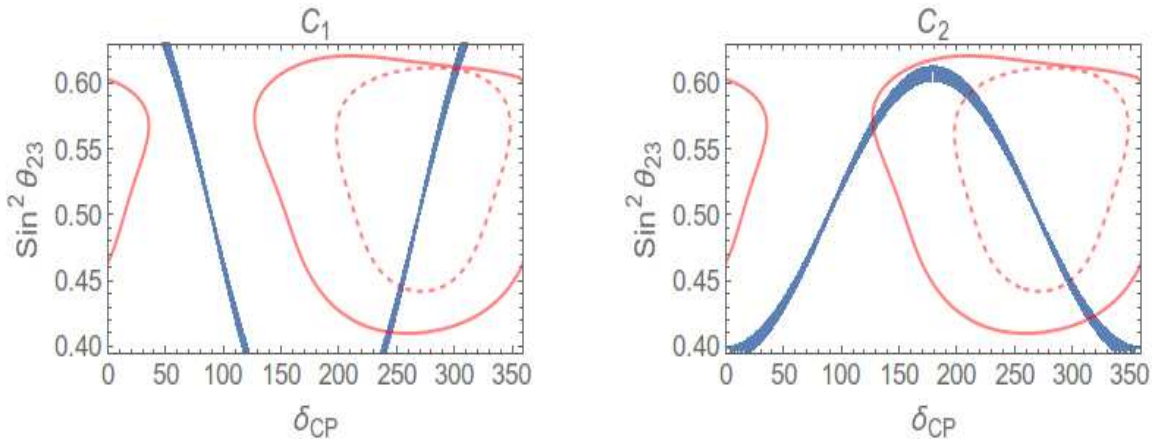


FIG. 1: The thick blue lines show the correlation plots in the $\sin^2 \theta_{23}$ - δ_{CP} plane as predicted by the symmetry relations. The left (right) panel correspond to Eq.(4) (Eq.(5)). The solid(dashed) red curves represent the 3σ allowed parameter space as obtained by the global analysis of data by the Nu-fit collaboration [34, 64] considering hierarchy to be NH(IH) respectively.

Fig. 1, shows the correlation plots between $\sin^2 \theta_{23}$ and δ_{CP} as given by eqs. (4, 5). These equations give two values of CP phase (namely, δ_{CP} and $360^\circ - \delta_{CP}$) for each value of θ_{23} except for $\delta_{CP} \equiv 180^\circ$. The width of the lines are due to the uncertainty of the angles θ_{12} and θ_{13} subject to the conditions $s_{12}^2 c_{13}^2 = 1/3$ and $c_{12}^2 c_{13}^2 = 2/3$ corresponding to eq. (4) and eq. (5) respectively. It is seen that the correlation between $\sin^2 \theta_{23}$ and δ_{CP} is opposite in the class of symmetries that give eq. (4) vis-a-vis those that give eq. (5). The parameters, $\sin^2 \theta_{23}$ and δ_{CP} are correlated between $0^\circ - 180^\circ$ and anti-correlated between $180^\circ - 360^\circ$ for eq. (4). The opposite is true for eq. (5). We also notice here that eq. (5) rules out regions around CP conserving (i.e. $0^\circ, 180^\circ, 360^\circ$) values. The red solid(dashed) contours represent the 3σ allowed region for NH(IH) as obtained

from the global-fit data by the Nu-fit collaboration [64]. We observe that at 3σ some of the allowed regions of $\sin^2 \theta_{23}$ and δ_{CP} as predicted by the symmetries are disfavoured by the current global-fit data. From the global-fit data we observe that the region $39^\circ < \delta_{CP} < 125^\circ$ is completely ruled out at 3σ for NH and the region $\delta_{CP} < 195^\circ$ for IH. The symmetry predictions can further constrain the values of δ_{CP} presently allowed by the global data.

In the next section, we study how far the allowed areas in $\delta_{CP} - \sin^2 \theta_{23}$ plane can be restricted if the simulated experimental data confronts the symmetry predictions.

III. SPECIFICATIONS OF THE EXPERIMENTS

In this paper, we have simulated all the experiments using the GLoBES package [65, 66] along with the required auxiliary files [67, 68]. We have considered the experimental set-up and the detector performance of DUNE and HK in accordance with ref. [69] and ref. [70] respectively.

- **Deep Underground Neutrino Experiment (DUNE) :** DUNE is a Fermilab based next generation long baseline super-beam experiment. This experiment will utilize the existing NuMI (Neutrinos at the Main Injector) beamline design. In this experiment, the muon-neutrinos from Fermilab will travel a baseline of 1300 km before it gets detected at the far detector situated at the “Sanford Underground Research Facility (SURF)” in Lead, South Dakota. The proposed far detector for DUNE is a LArTPC (liquid argon time-projection chamber) detector with the volume of 40 kT. The beam power will be initially 1.2 MW and later will be increased to 2.3 MW [71]. In our simulation we consider the neutrino flux [72] corresponding to 1.2 MW beam power which gives 1×10^{21} protons on target (POT) per year. This corresponds to a proton energy of 120 GeV.
- **Hyper-Kamiokande Experiment :** Hyper-Kamiokande experiment [70] is a budding successor to the triumphant Super-Kamiokande experiment. The primary goal of this experiment is to determine CP violation. However, it is also capable of observing nucleon decay, atmospheric neutrinos and neutrinos of astronomical origin. It is a Japan based long-baseline neutrino oscillation experiment using J-PARC (Japan Proton Accelerator Research Complex) neutrino beam facility with two alternatives for the location of the far detector. The first one is T2HK (Tokai-to-Hyper-Kamiokande) which plans on constructing two water-cherenkov detectors (cylindrical tanks) of fiducial volume 187 kt at 295 km in Kamioka. Alternatively, T2HKK proposes to have one tank of 187 kt at 295 km in Kamioka and the other 187 kt tank at 1100 km in Korea [70]. In our simulations we have considered the off-axis angle (OAA) for this detector in Korea as 1.5° , proposed run time ratio to be 1:3 in neutrino and antineutrino modes (total run time - 10 years) and the proton beam power of 1.3 MW giving a total of 27×10^{21} protons on target (POT).

Osc. param.	True Values	Test Values
$\sin^2 2\theta_{13}$	0.085	0.07 – 0.1
$\sin^2 \theta_{12}$	0.306	Fixed
θ_{23}	$39^\circ - 51^\circ$	$39^\circ - 51^\circ$
Δm_{21}^2 (eV 2)	7.50×10^{-5}	Fixed
Δm_{31}^2 (eV 2)	2.50×10^{-3}	$(2.35 - 2.65) \times 10^{-3}$
δ_{CP}	$(0-360)^\circ$	Symmetry predictions

TABLE I: Values of Oscillation parameters that are considered in this study unless otherwise mentioned. We vary the true values of θ_{23} in the whole allowed range and marginalization for each $\theta_{23}^{\text{true}}$ is done over the full allowed range of θ_{23} . See text for more details.

IV. PHENOMENOLOGICAL ANALYSIS

In this section, we perform a phenomenological analysis exploring the possibility of probing the correlations C_1 and C_2 at DUNE, T2HK and T2HKK. This is discussed in terms of correlation plots in $\sin^2 \theta_{23} - \delta_{CP}$ plane. We also discuss the possibility of distinguishing between the two models at these experiments. We perform a χ^2 test with χ^2 defined as,

$$\chi^2 = \text{Min}[\chi_{\text{stat}}^2 + \chi_{\text{syst}}^2 + \chi_{\text{prior}}^2]. \quad (9)$$

We assume Poisson distribution to calculate the statistical χ^2_{stat} ,

$$\chi^2_{stat} = \sum_i 2(N_i^{test} - N_i^{true} - N_i^{true} \log \frac{N_i^{test}}{N_i^{true}}). \quad (10)$$

Here, ‘i’ refers to the number of bins and N_i^{test}, N_i^{true} are the total number of events due to test and true set of oscillation parameters respectively. In Table I, we list the values for the neutrino oscillation parameters that we have used in our numerical simulation. These values are consistent with the results obtained from global-fit of world neutrino data [32–34]. The systematic errors are taken into account using the method of pulls [73, 74] as outlined in [75]. The systematic uncertainties (normalization errors) and efficiencies corresponding to signals and backgrounds of DUNE and HK are taken from [42, 70]. For DUNE the signal normalization uncertainties on $\nu_e/\bar{\nu}_e$ and $\nu_\mu/\bar{\nu}_\mu$ are considered to be 2% and 5% respectively. While a range of 5% to 20% background uncertainty along with the correlations among their sources have also been included. On the other hand, for T2HK and T2HKK the signal normalization error on $\nu_e(\bar{\nu}_e)$ and $\nu_\mu(\bar{\nu}_\mu)$ are considered to be 3.2% (3.9%) and 3.6%(3.6%) respectively. The background normalization uncertainties range from 3.8% to 5%. Additionally, we have added 5% prior on $\sin^2 2\theta_{13}$ in our numerical simulation.

A. Testing the $\sin^2 \theta_{23} - \delta_{CP}$ correlation predicted by the symmetries at DUNE, T2HK and T2HKK

For this analysis we simulate the experimental data by considering the true values of oscillation parameters given in Table I. For each true combination, in the theoretical fit we marginalize over $\sin^2 \theta_{13}$, Δm_{31}^2 and $\sin^2 \theta_{23}$ in the range given in Table I. However, the δ_{CP} values in the fit are taken according to the predictions of symmetries. We consider both NH and IH separately in our analysis. Thus, the resultant plots in Fig. (2,3) show the extent to which these three experiments can test the correlations between the two yet undetermined variables $\sin^2 \theta_{23}$ and δ_{CP} in conjunction with the symmetry predictions. The blue, grey and the yellow bands in the fig. (2,3) represent 1σ , 2σ , 3σ regions in the $\sin^2 \theta_{23} - \delta_{CP}$ plane respectively and the red contours show the 3σ allowed area obtained by the Nu-fit collaboration [34, 64]. The topmost panel corresponds to DUNE - 40 kT detector whereas the middle and the lowest panels correspond to T2HK and T2HKK experiments respectively. The left plots in all the rows are for testing C_1 whereas the right plots are for testing C_2 .

The figures show that because of the correlations predicted by symmetries, certain combinations of the true θ_{23} and δ_{CP} values get excluded by DUNE, T2HK and T2HKK. Owing to their high sensitivity to determine CP violation, T2HK and T2HKK constrain the range of δ_{CP} better than that of DUNE. This can be seen from the figure (fig. 2,3) which shows that, as we go from top to bottom the contours gets thinner w.r.t δ_{CP} . For instance for the C_1 correlation, the CP conserving values 0 and 360° get excluded at 3σ for both the octants by all the three experiments as can be seen from the plots in the left panels. However, for the C_2 , these values are allowed at 3σ for all the three experiments. Whereas, $\delta_{CP} = 0^\circ$ and 360° are excluded by DUNE and HK experiments at 1σ and 2σ respectively. Again one can see from the right panels that for C_2 , $\delta_{CP} = 180^\circ$ is allowed for $\sin^2 \theta_{23} > 0.55$ (i.e. higher octant) by DUNE but gets barely excluded at 2σ by T2HK and T2HKK experiments. The correlations predicted by the symmetry considerations being independent of hierarchy, the allowed regions are not very different for NH and IH. But the region of parameter space allowed by current data for IH is more constrained and the symmetry predictions restrict it further. Some of the parameter space allowed by the current data can also be disfavoured by incorporating the correlations due to symmetry relations.

B. Differentiating between the C_1 and C_2 symmetries

In this subsection, we explore the possibility of differentiation between the C_1 and C_2 . This is presented in Fig. (4) where we plot $\Delta\chi^2$ vs true θ_{23} . To find χ^2_{stat} (eq.(10)), true events are calculated by spanning the true values of θ_{23} in the range ($39^\circ - 51^\circ$) with marginalization over $\sin^2 \theta_{12}$ and $\sin^2 \theta_{13}$, and the true δ_{CP} values are calculated using the C_1 , provided the conditions given in eqn.(8) are satisfied. The remaining oscillation parameters are kept fixed at their best-fit values as shown in Table (I). Thus two sets of true events are generated corresponding to δ_{CP} and $360^\circ - \delta_{CP}$. In the theoretical fit, to calculate test events, we marginalize over $\sin^2 \theta_{12}$, $\sin^2 \theta_{13}$, Δm_{31}^2 , $\sin^2 \theta_{23}$ in the range given in Table (I) and test δ_{CP} values are calculated using the C_2 . Here we are presenting the analysis considering the true hierarchy as NH, analysis was also done with true hierarchy as IH and we obtained similar results. The three panels from left to right represent DUNE, T2HK and T2HKK respectively. The solid blue curves in the plots are for predicted range $\delta_{CP} \in (0 < \delta_{CP} < 180^\circ)$ and the dashed blue curves in the plots are for complementary range $360^\circ - \delta_{CP} \in (180^\circ < \delta_{CP} < 360^\circ)$ as predicted by the correlations. Both plots are with known normal hierarchy. The brown solid lines show the 3σ line for correlation differentiation. We observe from the figure that at maximal θ_{23} both correlations are indistinguishable by all the three experiments as is expected from the equations (4,5). These equations show that at maximal θ_{23} both the correlations predict maximal δ_{CP} value. The capability of the experiments to differentiate between the two correlations increases as we move away from maximal value. The range of θ_{23} for which the three experiments

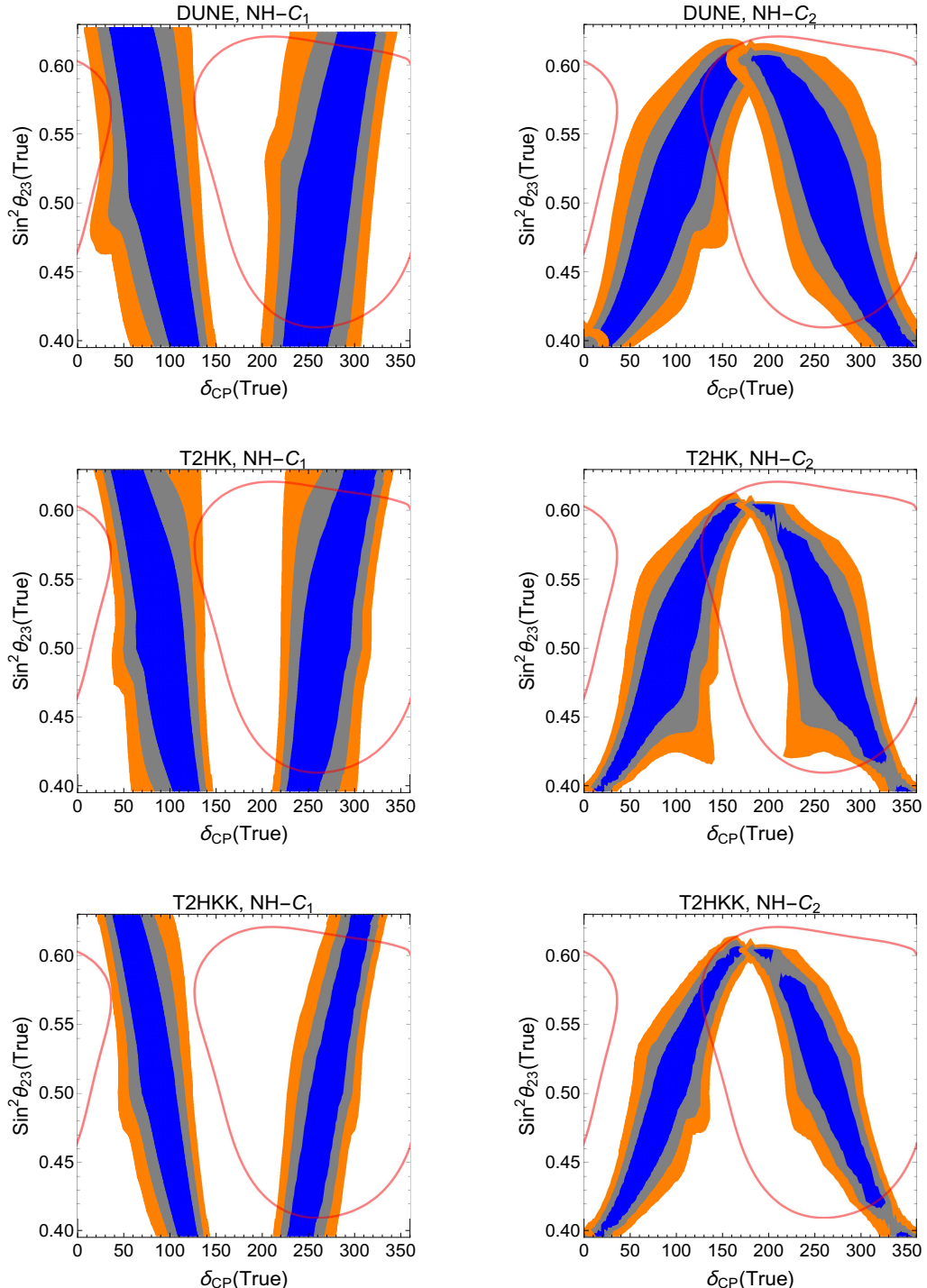


FIG. 2: Contour plots in the true: $\sin^2 \theta_{23}(\text{true})$ - $\delta_{CP}(\text{true})$ plane for DUNE, T2HK, T2HKK. The left(right) panels represent the predictions from the symmetry relations $C_1(C_2)$ which corresponds to the equations 4 (5) respectively. The hierarchy is fixed as NH. The red contour in each panel represent the 3σ allowed area from the global analysis of neutrino oscillation data as obtained by the Nu-fit collaboration [34, 64] for Normal Hierarchy. The blue, gray and yellow shaded contours correspond to 1σ , 2σ , 3σ respectively.

can differentiate between the correlations at 3σ is given in table II. The lower limits signify the values of θ_{23} below which the correlations can be differentiated at 3σ and the upper limits is for the values above which the same can be achieved.

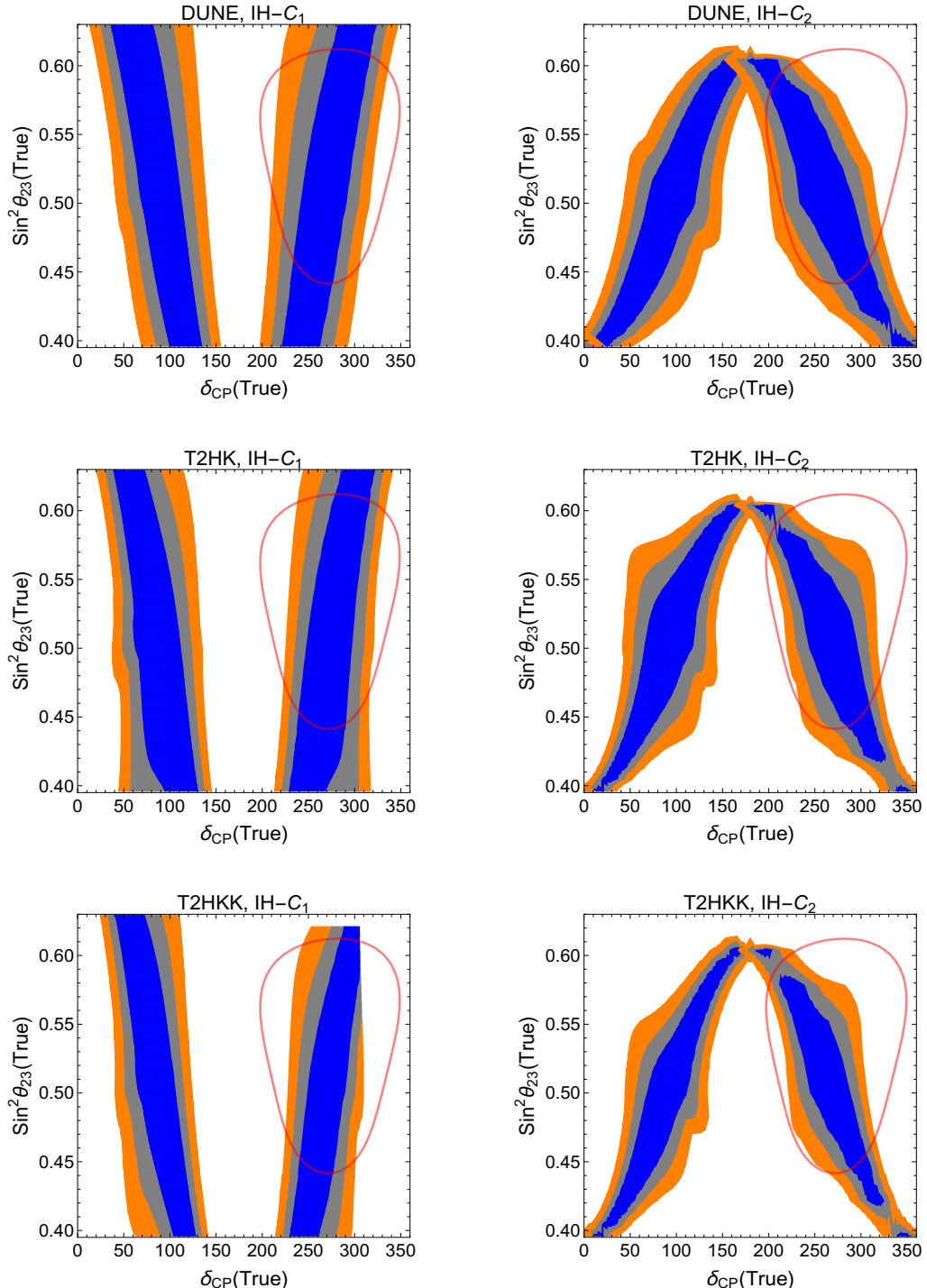


FIG. 3: Contour plots in the true: $\sin^2 \theta_{23}(\text{true})$ - $\delta_{CP}(\text{true})$ plane for DUNE, T2HK, T2HKK. The left(right) panels represent the predictions from the symmetry relations $C_1(C_2)$ which corresponds to the equations 4 (5) respectively. The hierarchy is fixed as IH. The red contour in each panel represent the 3σ allowed area from the global analysis of neutrino oscillation data as obtained by the Nu-fit collaboration [34, 64] for Inverted Hierarchy. The blue, gray and yellow shaded contours correspond to 1σ , 2σ , 3σ respectively.

V. CONCLUSION

We study here partial $\mu - \tau$ reflection symmetry of the leptonic mixing matrix, U , which can arise from discrete flavour symmetry. Specific assumptions which lead to this symmetry were reviewed here. This symmetry implies $|U_{\mu i}| = |U_{\tau i}|$ ($i = 1, 2, 3$) for a single column of the leptonic mixing matrix U . If this is true for the third column of U then it leads to maximal value of the atmospheric mixing angle and CP phase δ_{CP} . However, if this is true for the first or the second column then one obtains

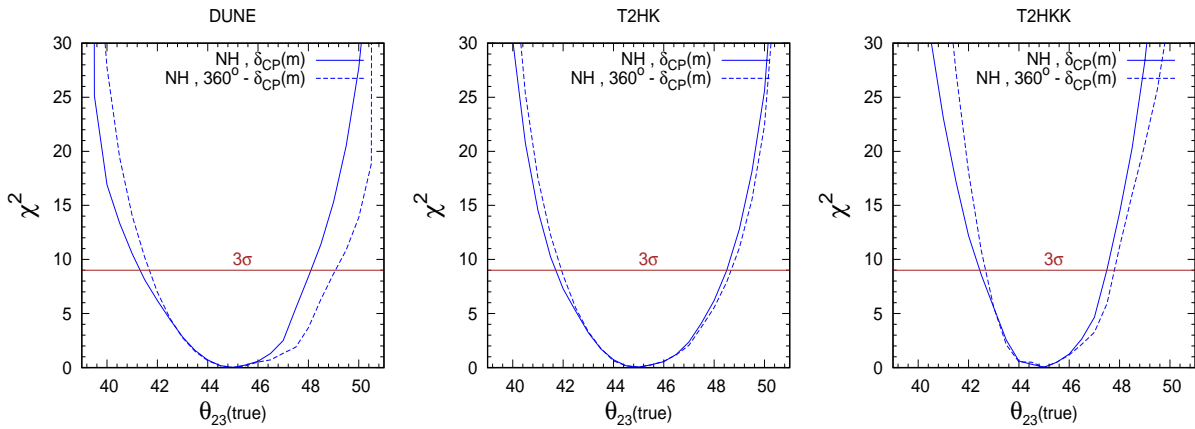


FIG. 4: The sensitivity of the DUNE, T2HK & T2HKK experiments to differentiate between C_1 and C_2 correlations for known normal hierarchy.

	DUNE		T2HK		T2HKK	
	δ_{CP}	$360^\circ - \delta_{CP}$	δ_{CP}	$360^\circ - \delta_{CP}$	δ_{CP}	$360^\circ - \delta_{CP}$
lower limit	41.5°	42°	42°	42°	42.5°	43°
upper limit	48°	49°	48°	48°	47.5°	48°

TABLE II: Values of θ_{23} in degrees above and below which the correlations C_1 and C_2 can be differentiated with minimum 3σ significance.

definite correlations among θ_{23} and δ_{CP} . We call these scenarios C_1 (equality for the first column) and C_2 (equality of the 2nd column). We find that almost all the discrete subgroups of $SU(3)$, except a few exceptional cases, having three dimensional irreducible representations display the form of partial $\mu - \tau$ symmetry. We study the correlations among θ_{23} and δ_{CP} in the two scenarios. Each scenario gives two values of δ_{CP} for a given θ_{23} – one belonging to $0 < \delta_{CP} < 180^\circ$ and the other belonging to $180^\circ < \delta_{CP} < 360^\circ$. The models also give specific correlations between θ_{23} and δ_{CP} and these are opposite for C_1 and C_2 . We study how the allowed areas in the $\sin^2 \theta_{23} - \delta_{CP}$ plane obtained by the global analysis of neutrino oscillation data from the Nu-Fit collaboration compare with the predictions from the symmetries.

We also expound the testability of these symmetries considering next generation accelerator based experiments, DUNE and Hyper-Kamiokande. This is illustrated in terms of plots in the $\sin^2 \theta_{23}$ (true) - δ_{CP} (true) plane obtained by fitting the simulated experimental data with the symmetry predictions for δ_{CP} . The values of θ_{23} are found to be more constrained for the CP conserving values namely $\delta_{CP} = 0, 180^\circ, 360^\circ$. For the C_2 correlation, the θ_{23} is found to be in the higher octant for $\delta_{CP} = 180^\circ$ and in the lower octant for $\delta_{CP} = 0$ and 360° . For the correlation C_1 , values of δ_{CP} around all the three CP conserving values $\delta_{CP} = 0, 180^\circ$ and 360° are seen to be disfavoured. Finally, we illustrate the capability of DUNE and Hyper-Kamiokande to distinguish between the predictions of the two correlations. We observe that both the experiments can better differentiate between these two as one moves away from the maximal θ_{23} value.

In conclusion, the future experiments provide testing grounds for various symmetry relations, specially those connecting θ_{23} and δ_{CP} .

Acknowledgments

The research work of ASJ was supported by BRNS (Department of Atomic Energy) and by Department of Science and Technology, Government of India through the Raja Ramanna fellowship and the J. C. Bose grant respectively. NN gratefully acknowledges the support in part by the National Natural Science Foundation of China under grant No.11775231 for the research

work.

[1] Guido Altarelli and Ferruccio Feruglio. Discrete Flavor Symmetries and Models of Neutrino Mixing. *Rev. Mod. Phys.*, 82:2701–2729, 2010.

[2] Guido Altarelli, Ferruccio Feruglio, and Luca Merlo. Tri-Bimaximal Neutrino Mixing and Discrete Flavour Symmetries. *Fortsch. Phys.*, 61:507–534, 2013.

[3] Alexei Yu. Smirnov. Discrete symmetries and models of flavor mixing. *J. Phys. Conf. Ser.*, 335:012006, 2011.

[4] Hajime Ishimori, Tatsuo Kobayashi, Hiroshi Ohki, Yusuke Shimizu, Hiroshi Okada, and Morimitsu Tanimoto. Non-Abelian Discrete Symmetries in Particle Physics. *Prog. Theor. Phys. Suppl.*, 183:1–163, 2010.

[5] Stephen F. King and Christoph Luhn. Neutrino Mass and Mixing with Discrete Symmetry. *Rept. Prog. Phys.*, 76:056201, 2013.

[6] P. F. Harrison and W. G. Scott. mu - tau reflection symmetry in lepton mixing and neutrino oscillations. *Phys. Lett.*, B547:219–228, 2002.

[7] Walter Grimus and Luis Lavoura. A Nonstandard CP transformation leading to maximal atmospheric neutrino mixing. *Phys. Lett.*, B579:113–122, 2004.

[8] P. M. Ferreira, W. Grimus, L. Lavoura, and P. O. Ludl. Maximal CP Violation in Lepton Mixing from a Model with Delta(27) flavour Symmetry. *JHEP*, 09:128, 2012.

[9] Walter Grimus and Luis Lavoura. mu-tau Interchange symmetry and lepton mixing. *Fortsch. Phys.*, 61:535–545, 2013.

[10] R. N. Mohapatra and C. C. Nishi. S_4 Flavored CP Symmetry for Neutrinos. *Phys. Rev.*, D86:073007, 2012.

[11] Ernest Ma, Alexander Natale, and Oleg Popov. Neutrino Mixing and CP Phase Correlations. *Phys. Lett.*, B746:114–116, 2015.

[12] Anjan S. Joshipura and Ketan M. Patel. Generalized μ - τ symmetry and discrete subgroups of $O(3)$. *Phys. Lett.*, B749:159–166, 2015.

[13] Anjan S. Joshipura. Neutrino masses and mixing from flavour antisymmetry. *JHEP*, 11:186, 2015.

[14] Anjan S Joshipura and Newton Nath. Neutrino masses and mixing in A_5 with flavor antisymmetry. *Phys. Rev.*, D94(3):036008, 2016.

[15] C. C. Nishi and B. L. Sanchez-Vega. Mu-tau reflection symmetry with a texture-zero. *JHEP*, 01:068, 2017.

[16] Zhen-hua Zhao. Breakings of the neutrino $\mu - \tau$ reflection symmetry. *JHEP*, 09:023, 2017.

[17] Zhi-Cheng Liu, Chong-Xing Yue, and Zhen-hua Zhao. Neutrino $\mu - \tau$ reflection symmetry and its breaking in the minimal seesaw. *JHEP*, 10:102, 2017.

[18] Zhi-zhong Xing, Di Zhang, and Jing-yu Zhu. The $\mu - \tau$ reflection symmetry of Dirac neutrinos and its breaking effect via quantum corrections. 2017.

[19] Zhi-zhong Xing and Jing-yu Zhu. Neutrino mass ordering and $\mu - \tau$ reflection symmetry breaking. 2017.

[20] Anjan S. Joshipura. Perturbed flavour symmetries and predictions of CP violating phase δ . 2018.

[21] Newton Nath, Zhi-zhong Xing, and Jue Zhang. $\mu - \tau$ Reflection Symmetry Embedded in Minimal Seesaw. 2018.

[22] Zhen-hua Zhao. Modifications to the neutrino mixing given by the mu-tau reflection symmetry. 2018.

[23] C. Patrignani et al. Review of Particle Physics. *Chin. Phys.*, C40(10):100001, 2016.

[24] Takeshi Fukuyama and Hiroyuki Nishiura. Mass matrix of Majorana neutrinos. 1997.

[25] Ernest Ma and Martti Raidal. Neutrino mass, muon anomalous magnetic moment, and lepton flavor nonconservation. *Phys. Rev. Lett.*, 87:011802, 2001. [Erratum: *Phys. Rev. Lett.* 87, 159901(2001)].

[26] C. S. Lam. A 2-3 symmetry in neutrino oscillations. *Phys. Lett.*, B507:214–218, 2001.

[27] K. R. S. Balaji, W. Grimus, and T. Schwetz. The Solar LMA neutrino oscillation solution in the Zee model. *Phys. Lett.*, B508:301–310, 2001.

[28] Walter Grimus, Anjan S. Joshipura, Satoru Kaneko, Luis Lavoura, Hideyuki Sawanaka, and Morimitsu Tanimoto. Non-vanishing $U(e3)$ and $\cos 2 \theta(23)$ from a broken $Z(2)$ symmetry. *Nucl. Phys.*, B713:151–172, 2005.

[29] Anjan S. Joshipura. Universal 2-3 symmetry. *Eur. Phys. J.*, C53:77–85, 2008.

[30] Zhi-zhong Xing and Zhen-hua Zhao. A review of - flavor symmetry in neutrino physics. *Rept. Prog. Phys.*, 79(7):076201, 2016.

[31] K. Abe et al. Combined Analysis of Neutrino and Antineutrino Oscillations at T2K. *Phys. Rev. Lett.*, 118(15):151801, 2017.

[32] P. F. de Salas, D. V. Forero, C. A. Ternes, M. Tortola, and J. W. F. Valle. Status of neutrino oscillations 2017. 2017.

[33] F. Capozzi, E. Lisi, A. Marrone, D. Montanino, and A. Palazzo. Neutrino masses and mixings: Status of known and unknown 3ν parameters. *Nucl. Phys.*, B908:218–234, 2016.

[34] Ivan Esteban, M. C. Gonzalez-Garcia, Michele Maltoni, Ivan Martinez-Soler, and Thomas Schwetz. Updated fit to three neutrino mixing: exploring the accelerator-reactor complementarity. 2016.

[35] Zhi-zhong Xing and Shun Zhou. A partial symmetry and its prediction for leptonic CP violation. *Phys. Lett.*, B737:196–200, 2014.

[36] Shao-Feng Ge, Duane A. Dicus, and Wayne W. Repko. Z_2 Symmetry Prediction for the Leptonic Dirac CP Phase. *Phys. Lett.*, B702:220–223, 2011.

[37] Shao-Feng Ge, Duane A. Dicus, and Wayne W. Repko. Residual Symmetries for Neutrino Mixing with a Large θ_{13} and Nearly Maximal δ_D . *Phys. Rev. Lett.*, 108:041801, 2012.

[38] S. T. Petcov. Discrete Flavour Symmetries, Neutrino Mixing and Leptonic CP Violation. 2017.

[39] Reinier de Adelhart Toorop, Ferruccio Feruglio, and Claudia Hagedorn. Discrete Flavour Symmetries in Light of T2K. *Phys. Lett.*, B703:447–451, 2011.

[40] Andrew D. Hanlon, Shao-Feng Ge, and Wayne W. Repko. Phenomenological consequences of residual \mathbb{Z}_2^s and $\overline{\mathbb{Z}}_2^s$ symmetries. *Phys. Lett.*, B729:185–191, 2014.

[41] Andrew D. Hanlon, Wayne W. Repko, and Duane A. Dicus. Residual Symmetries Applied to Neutrino Oscillations at NOvA and T2K. *Adv. High Energy Phys.*, 2014:469572, 2014.

[42] R. Acciarri et al. Long-Baseline Neutrino Facility (LBNF) and Deep Underground Neutrino Experiment (DUNE). 2015.

[43] Vernon Barger, Atri Bhattacharya, Animesh Chatterjee, Raj Gandhi, Danny Marfatia, et al. Configuring the Long-Baseline Neutrino Experiment. *Phys. Rev.*, D89(1):011302, 2014.

[44] Sanjib Kumar Agarwalla, Suprabh Prakash, and S. Uma Sankar. Exploring the three flavor effects with future superbeams using liquid argon detectors. *JHEP*, 1403:087, 2014.

[45] Vernon Barger, Atri Bhattacharya, Animesh Chatterjee, Raj Gandhi, Danny Marfatia, and Mehedi Masud. Optimal configurations of the Deep Underground Neutrino Experiment. *Int. J. Mod. Phys.*, A31(07):1650020, 2016.

[46] Kalpana Bora, Debajyoti Dutta, and Pomita Ghoshal. Determining the octant of θ_{23} at LBNE in conjunction with reactor experiments. *Mod. Phys. Lett.*, A30(14):1550066, 2015.

[47] Monojit Ghosh, Srubabati Goswami, and Sushant K. Raut. Maximizing the DUNE early physics output with current experiments. *Eur. Phys. J.*, C76(3):114, 2016.

[48] Debajyoti Dutta and kalpana Bora. Probing CP violation at LBNE with reactor experiments. *Mod. Phys. Lett.*, A30(07):1550017, 2015.

[49] K. N. Deepthi, C. Soumya, and R. Mohanta. Revisiting the sensitivity studies for leptonic CP-violation and mass hierarchy with T2K, NOvA and LBNE experiments. *New J. Phys.*, 17(2):023035, 2015.

[50] Newton Nath, Monojit Ghosh, and Srubabati Goswami. The physics of antineutrinos in DUNE and determination of octant and δ_{CP} . *Nucl. Phys.*, B913:381–404, 2016.

[51] Rahul Srivastava, Christoph A. Ternes, Mariam Trtola, and Jos W. F. Valle. Zooming in on neutrino oscillations with DUNE. 2018.

[52] Pedro Pasquini. Review: Long-baseline oscillation experiments as a tool to probe High Energy Models. 2018.

[53] Rahul Srivastava, C. A. Ternes, M. Trtola, and J. W. F. Valle. Testing a lepton quarticity flavor theory of neutrino oscillations with the DUNE experiment. *Phys. Lett.*, B778:459–463, 2018.

[54] Sanjib Kumar Agarwalla, Sabya Sachi Chatterjee, S. T. Petcov, and A. V. Titov. Addressing Neutrino Mixing Schemes with DUNE and T2HK. 2017.

[55] Sabya Sachi Chatterjee, Mehedi Masud, Pedro Pasquini, and J. W. F. Valle. Cornering the revamped BMV model with neutrino oscillation data. *Phys. Lett.*, B774:179–182, 2017.

[56] S. T. Petcov and A. V. Titov. Assessing the Viability of A_4 , S_4 and A_5 Flavour Symmetries for Description of Neutrino Mixing. 2018.

[57] Peter Ballett, Stephen F. King, Silvia Pascoli, Nick W. Prouse, and TseChun Wang. Precision neutrino experiments vs the Littlest Seesaw. *JHEP*, 03:110, 2017.

[58] Peter Ballett, Silvia Pascoli, and Jessica Turner. Mixing angle and phase correlations from A5 with generalized CP and their prospects for discovery. *Phys. Rev.*, D92(9):093008, 2015.

[59] Peter Ballett, Stephen F. King, Christoph Luhn, Silvia Pascoli, and Michael A. Schmidt. Testing solar lepton mixing sum rules in neutrino oscillation experiments. *JHEP*, 12:122, 2014.

[60] J. T. Penedo, S. T. Petcov, and T. Yanagida. Low-Scale Seesaw and the CP Violation in Neutrino Oscillations. *Nucl. Phys.*, B929:377–396, 2018.

[61] Stephen F. King and Thomas Neder. Lepton mixing predictions including Majorana phases from $(6n^2)$ flavour symmetry and generalised CP. *Phys. Lett.*, B736:308–316, 2014.

[62] Anjan S. Joshipura and Ketan M. Patel. Residual Z_2 symmetries and leptonic mixing patterns from finite discrete subgroups of $U(3)$. *JHEP*, 01:134, 2017.

[63] Walter Grimus and Patrick Otto Ludl. On the characterization of the $SU(3)$ -subgroups of type C and D. *J. Phys.*, A47(7):075202, 2014.

[64] NuFIT 3.2 (2018), <http://www.nu-fit.org/>.

[65] Patrick Huber, M. Lindner, and W. Winter. Simulation of long-baseline neutrino oscillation experiments with GLoBES. *Comput. Phys. Commun.*, 167:195, 2005.

[66] Patrick Huber, Joachim Kopp, Manfred Lindner, Mark Rolinec, and Walter Winter. New features in the simulation of neutrino oscillation experiments with GLoBES 3.0. *Comput. Phys. Commun.*, 177:432–438, 2007.

[67] Mark D. Messier. Evidence for neutrino mass from observations of atmospheric neutrinos with Super-Kamiokande. 1999. Ph.D. Thesis (Advisor: James L. Stone).

[68] E.A. Paschos and J.Y. Yu. Neutrino interactions in oscillation experiments. *Phys. Rev.*, D65:033002, 2002.

[69] T. Alion et al. Experiment Simulation Configurations Used in DUNE CDR. 2016.

[70] K. Abe et al. Physics Potentials with the Second Hyper-Kamiokande Detector in Korea. 2016.

[71] C. Adams et al. Scientific Opportunities with the Long-Baseline Neutrino Experiment. 2013.

[72] Daniel Cherdack. . 2014.

[73] M. C. Gonzalez-Garcia and Michele Maltoni. Atmospheric neutrino oscillations and new physics. *Phys. Rev.*, D70:033010, 2004.

[74] G.L. Fogli, E. Lisi, A. Marrone, D. Montanino, and A. Palazzo. Getting the most from the statistical analysis of solar neutrino oscillations. *Phys. Rev.*, D66:053010, 2002.

[75] Raj Gandhi et al. Mass Hierarchy Determination via future Atmospheric Neutrino Detectors. *Phys. Rev.*, D76:073012, 2007.